Annales Geophysicae (2002) 20: 1499–1507

Annales Geophysicae

Electron acceleration observed by the FAST satellite within the IAR during a 3 Hz modulated EISCAT heater experiment

S. R. Cash[1], **J. A. Davies**[1], **E. Kolesnikova**[1], **T. R. Robinson**[1], **D. M. Wright**[1], **T. K. Yeoman**[1], **and R. J. Strangeway**[2]

[1]Department of Physics and Astronomy, University of Leicester, University Road, Leicester LE1 7RH, UK
[2]University of California, Institute of Geophysics and Planetary Physics, 405 Hilgard Ave., Los Angeles CA 90095, USA

Received: 7 February 2002 – Revised: 3 July 2002 – Accepted: 17 July 2002

Abstract. A quantitative analysis is presented of the FAST satellite electric field and particle flux data during an EISCAT heating experiment run on 8 October 1998. Radio frequency heating, modulated at 3 Hz, launched ULF waves from the ionosphere into the lower magnetosphere. The ULF waves were observed in FAST data and constituted the first satellite detection of artificially excited Alfvénic ULF waves. The downward electron flux data for this event contain the first observations of electrons undergoing acceleration within the Ionospheric Alfvén Resonator (IAR) due to parallel electric fields associated with an artificially stimulated Alfvén wave. The time history and spectral content of the observed downward electron fluxes is investigated by considering the effects of a localised parallel electric field. Furthermore, it is demonstrated that a power law electron energy distribution describes the time-variable observed fluxes better than a Maxwellian distribution.

Key words. Ionosphere (active experiments; particle acceleration) – Magnetospheric physics (electric fields)

1 Introduction

It is increasingly understood that Alfvén waves play an important role in coupling the magnetosphere and the ionosphere. In particular, observations from auroral sounding rockets and various satellites have established Alfvén waves as being responsible for the acceleration of charged particles along geomagnetic field lines, which results in auroral precipitation. For example, Ivchenko et al. (1999) reported a quasi-periodic structure in magnetic field, electric field and particle flux data from the Auroral Turbulence II sounding rocket as it crossed the border of an auroral arc. Their analysis indicated that an Alfvén wave of small transverse scale had caused field-aligned precipitation. Furthermore, Chaston et al. (1999, 2000) found that Alfvén waves observed by the FAST satellite were directly associated with dispersed electron signatures in the dayside auroral oval.

Recently, an ionospheric heating experiment utilising the European Incoherent SCATter radar (EISCAT) high power facility at Tromsø, Norway, was run in order to investigate the link between Alfvén waves and the acceleration of precipitating field-aligned particles in an active manner. Results from this experiment have been reported in papers by Robinson et al. (2000) and Kolesnikova et al. (2002). In these reports, the particle acceleration process was explained by consideration of the properties of Alfvén waves within the Ionospheric Alfvén Resonator (IAR). The IAR is the term given to the vertical structure associated with the decay in plasma density going from the ionosphere into the magnetosphere, causing trapping of shear Alfvén waves due to the resulting large Alfvén velocity gradient. The lower boundary of the IAR in the ionosphere can be taken as the altitude where the angular frequency of the Alfvén wave matches the ion-neutral collision frequency (Borisov and Stubbe, 1997), whereas the upper boundary corresponds to where the Alfvén waves of interest undergo partial reflection. This occurs at an altitude somewhat below that where the Alfvén velocity maximises. Due to electron inertial effects, an Alfvén wave acquires a significant parallel electric field component near the upper IAR boundary (Lysak, 1993; Robinson et al., 2000). This electric field may effectively accelerate suprathermal electrons.

The EISCAT high power facility (heater) at Tromsø, Norway has been used since 1980 to generate artificial magnetic pulsations via modulated HF heating of the ionosphere (Stubbe et al., 1977, 1982). There have also been observations of heater-induced electromagnetic VLF waves by spacecraft (James et al., 1990; Kimura et al., 1994). However, the results from an experiment on 8 October 1998 reported by Robinson et al. (2000) represent the first spacecraft detection of artificially excited ULF waves. Furthermore, the observed downward electron fluxes constitute the first direct evidence for electron acceleration in the IAR by an artificially stimulated Alfvén wave.

Correspondence to: S. R. Cash (srcash@ion.le.ac.uk)

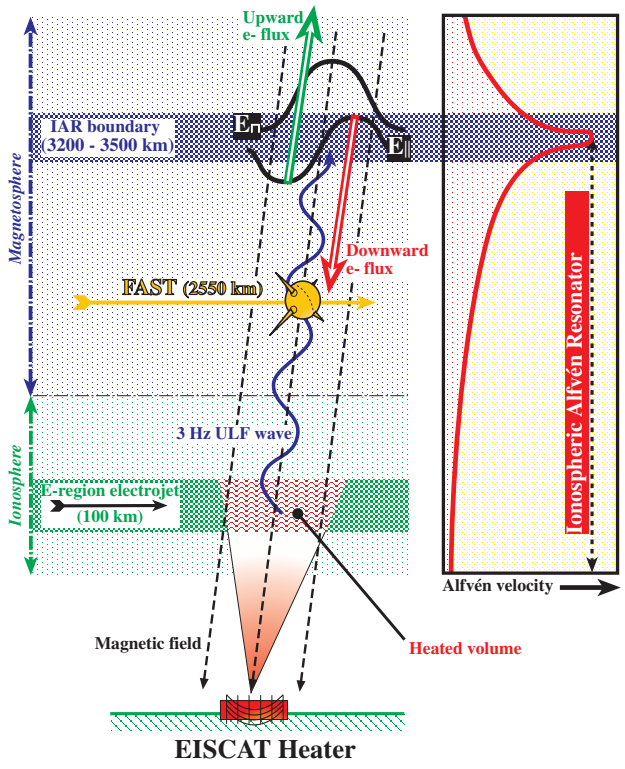

Fig. 1. Schematic showing the EISCAT heater modulating the conductivity in the E-region ionosphere where naturally occurring currents such as the electrojet are modulated by the heating modulation frequency of 3 Hz. This launches a 3 Hz ULF wave along the geomagnetic field lines that is detected directly by the FAST satellite. At the IAR the wave acquires a significant parallel electric field, which accelerates the downward moving electrons that are detected by FAST at each edge of the wave propagation region (after Robinson et al. 2000).

Following on from the initial report by Robinson et al. (2000), in a second paper, Kolesnikova et al. (2002) modelled the Alfvén wave field in the inhomogeneous plasma along a field line from the lower ionosphere, where the modulated heating takes place, up into the magnetosphere, beyond the altitude of the FAST satellite. Using the modelled wave fields, Kolesnikova et al. (2002) also made a preliminary attempt to account for the observed electron flux oscillations by assuming Maxwellian particle distributions. This was only partially successful. In the present paper, attention is focused on examining the spectral components in the data, and explaining the time history of the observed downward electron fluxes in further detail. We use the values of the modelled electric field in Kolesnikova et al. (2002) to investigate the effects of a localised parallel electric field on the electron energy distribution. Furthermore, it is demonstrated that a power law electron energy distribution describes the time-variable observed fluxes better than a Maxwellian distribution.

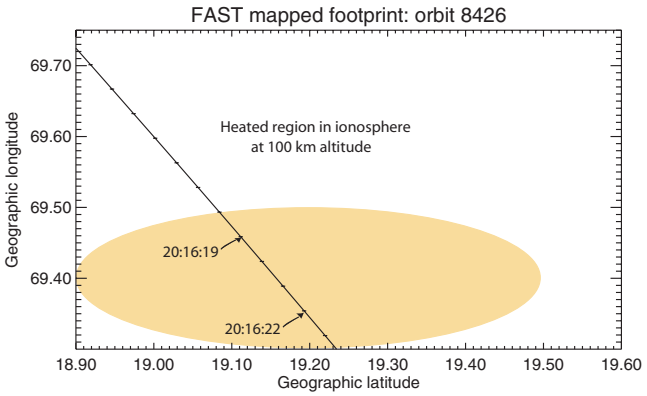

Fig. 2. FAST satellite track mapped from 2550 km altitude down the field lines (using IGRF Tysganenko 1989 model) to 100 km altitude. The shaded region represents the approximately circular heated region (3 dB level) at this altitude in the E-region ionosphere. The ticks mark each second of data; the arrows show times when a 3 Hz signal was observed in the FAST data shown in Fig. 3.

2 Experimental conditions

On 8 October 1998, between 20:15 UT and 20:45 UT, the EISCAT heater transmitted 4.04 MHz X-mode polarised radio waves into a cone of half-width 7° (at 3 dB level), centred along the direction of the local magnetic field. The HF signal was modulated by a square wave with a fundamental frequency of 3 Hz and an effective radiated power of 144 MW. This produced a heated layer a few km thick with an approximately circular cross section of 25 km diameter at an altitude of about 80 km. This layer acted as the source for the ULF waves (Robinson et al., 2000; Kolesnikova et al., 2002). This experimental arrangement forms part of the schematic illustration in Fig. 1. The location of Tromsø (69.6° N, 19.2° E in geographic coordinates) is within the auroral oval, and EISCAT UHF data during this experiment (see below for further details) indicated the presence of a significant electrojet current within the heated volume. The modulation of the heater power caused a modulation in the electrical conductivity at the same frequency. Thus, natural electrojet currents were modulated and acted as a source of ULF waves, which propagated up the magnetic field line. The heated region in the ionosphere defines the spatial extent of the flux tube which carries the ULF wave energy.

The FAST (Fast Auroral SnapshoT) satellite orbits the Earth at altitudes between 350 km and 4175 km at 83° inclination (Carlson et al., 1998). It has proved ideal for investigating the low altitude auroral acceleration region due to its high spatial and temporal resolution. Just after 20:16 UT, FAST passed over Tromsø at an altitude of approximately 2550 km. Figure 2 shows the spacecraft's mapped magnetic footprint (using the IGRF model) down to 100 km altitude. The two arrows indicate approximately the start and end of the period during which the FAST electric field sensors registered the signature of the ULF wave excited by the EISCAT heater. The shaded patch in the ionosphere shown on Fig. 2,

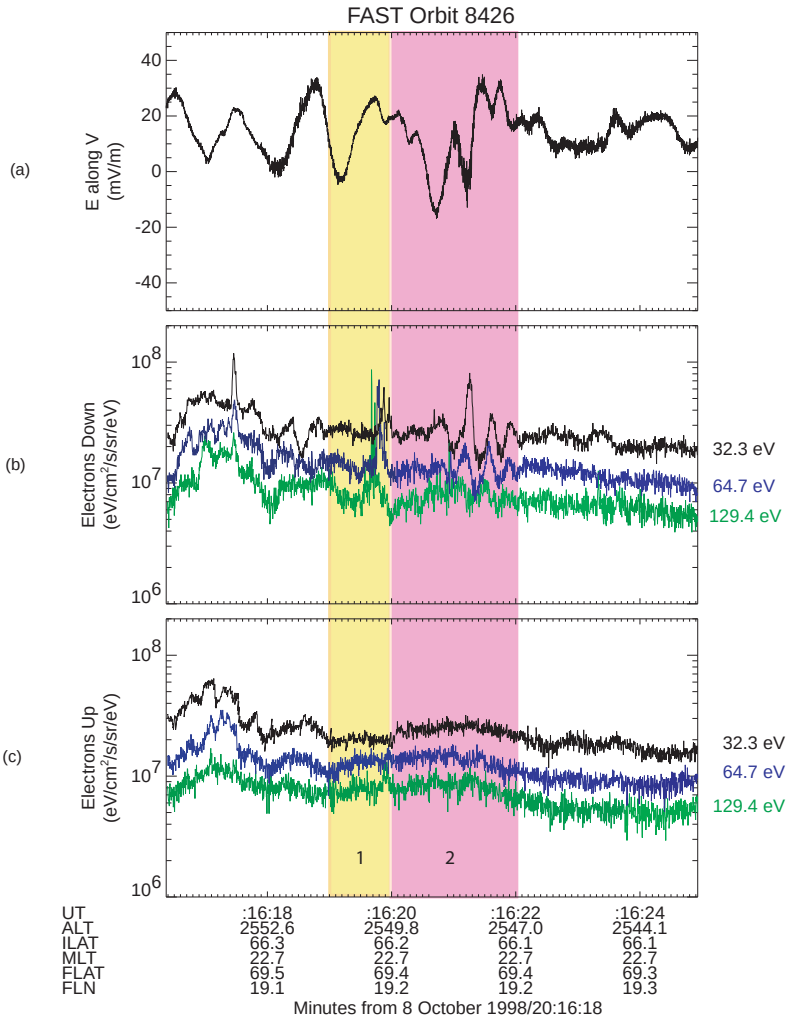

Fig. 3. FAST satellite data from 8 October 1998. Panel **(a)** shows an electric field component perpendicular to the magnetic field. Panels **(b)** and **(c)** show electron flux measured by the 32.3, 64.7 and 129.4 eV channels of the SESA instrument directed downward and upward, respectively, with units of fluxes multiplied by the centre energy of the corresponding energy channel (after Robinson et al., 2000).

centred at 69.4° latitude, represents the heated ionospheric region present when the EISCAT heater points in the field-aligned direction 12° from vertical. The electric field component measured by the FAST instrument was oriented nearly perpendicular to the magnetic field (Carlson et al., 1998; Robinson et al., 2000) and exhibits 3 Hz oscillations (see below for further details) from about 20:16:20 to 20:16:23 UT, with an amplitude of approximately 2–5 mV m^{-1}. These data are shown in panel (a) of Fig. 3. The interval of approximately 3–4 s in which 3 Hz oscillations were observed in the FAST instrument data is remarkably consistent with the expected size and location of the flux tube generated by the modulated heating regime. It should be noted that the agreement originally reported by Robinson et al. (2000) was somewhat less good than that described here. This was due to a slight error in the original mapping calculation that has since been rectified. It is also clear from Fig. 3 that lower (than 3 Hz) frequency oscillations of significant amplitude were present outside the interval of the artificial event. These oscillations are almost certainly natural in origin and are not connected with the EISCAT heater.

The differential electron energy flux (DEF) data shown in panels (b) and (c) of Fig. 3 are from FAST's Stepped Electrostatic Analyser (SESA) instruments, which operate as spectrographs to take high time resolution (1.7 ms) electron measurements in 16 pitch-angle bins (Carlson et al., 1998). Panel (b) contains the downward fluxes, while the corresponding upward fluxes are displayed in panel (c). The DEF energy channels shown are those from the three lowest energies, which have central energies of 32.3, 64.7 and 129.4 eV. These differential energy fluxes originated from particles with trajectories in directions that were within 30° of the magnetic field direction. Clear signatures of 3 Hz oscillations in the downward fluxes are present, within roughly the same interval when 3 Hz electric field oscillations appear. However, crucially, no significant 3 Hz oscillations appear in the upward fluxes. These data provide unambiguous evidence for electron acceleration from above the FAST spacecraft in the flux tube, which maps to the heated volume, as discussed in detail by Robinson et al. (2000). However, the temporal structure of the 3 Hz signatures is somewhat complicated and will be discussed in more detail in the next section. In order to facilitate this more detailed discussion, the time series has been divided into two specific time intervals, which

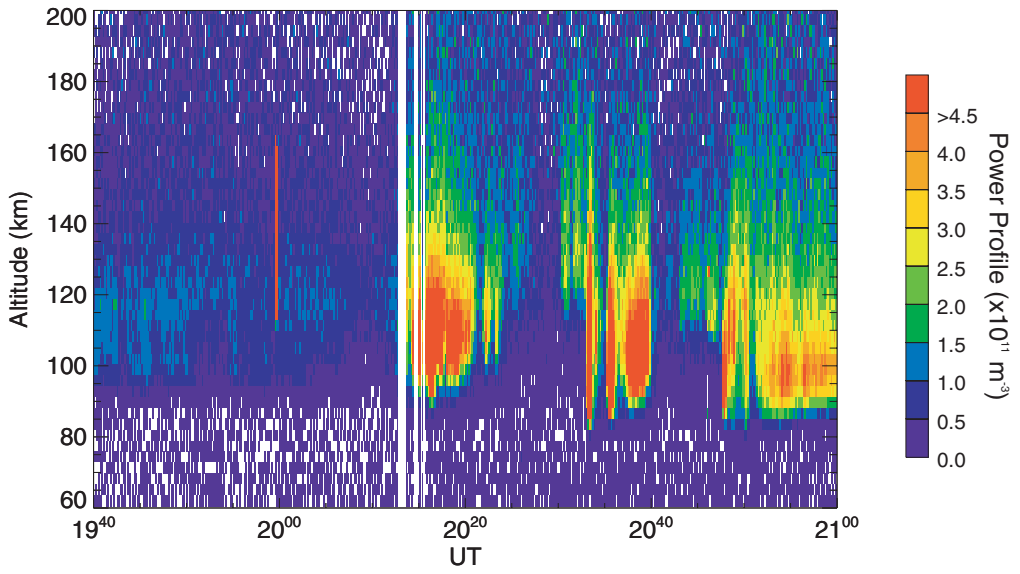

Fig. 4. Power Profile from EISCAT UHF radar for 8 October 1998, 3.1 km resolution with 10 s integration.

are indicated by coloured strips in Fig. 3. The yellow strip marks interval 1, which is from 20:16:19 to 20:16:20 UT; the pink strip marks interval 2, from 20:16:20 to 20:16:22 UT. The whole time interval corresponding to the combination of intervals 1 and 2 is identical to the time between the arrows in Fig. 2. Interval 2 contains the clearest signature of the 3 Hz oscillations in the downward electron flux (panel b). The 3 Hz signature in the electric field extends throughout intervals 1 and 2. Interval 1 does contain a signature of a disturbance in the downward flux, but it is difficult to discern a clear oscillatory pattern. One important feature of the downward flux data which is clearly exhibited in Fig. 3, and which has played an essential feature in the interpretation of the event, is the energy dispersion. These data exhibit time shifts between the peaks in the separate energy channels for both intervals 1 and 2. This feature strongly suggests that both of these enhanced flux features originate in acceleration processes above the satellite. Robinson et al. (2000) explained the origin of the two separated flux enhancement events in terms of cross-field gradients in the region of enhanced conductivity (see also the schematic illustration in Fig. 1). If this region were a Gaussian, intervals 1 and 2 should be reasonably similar. The reason for their asymmetry is not well understood at present. A possible explanation may be that the gradients first encountered by the FAST spacecraft (interval 1) may be steeper than those encountered during the exit from the heated region (interval 2). This might be due, for example, to the field-aligned geometry of the heater beam which gives rise to a narrower intersection region between the northern edge of the beam and the heated ionospheric layer than that at the southern edge where the spacecraft exits (see Fig. 1). This is consistent with the relatively shorter duration of interval 1 and would explain why no clear 3 Hz signature was identifiable, since it lasted for a time shorter than a wave period. It is also instructive to note that the strong burst of flux activity prior to interval 1 exhibits no energy dispersion and consequently, is not attributable to spatially and temporally localised acceleration from above the spacecraft.

Supporting ground-based observations during the heating experiment were also made by the EISCAT UHF radar (Rishbeth and Williams, 1985). The SP-UK-HEAT experiment on 8 October 1998 included UHF radar operation, with the transmit/receive antenna at Tromsø aligned along the local magnetic field direction (geographic azimuth: 183.2°, elevation: 77.2°) and the remote site UHF receivers at Kiruna, Sweden (67.9° N, 20.4° E) and Sodankylä, Finland (67.4° N, 26.6° E), intersecting the transmitter beam at the F-region altitude of 250 km. Four pulse schemes were transmitted: a long pulse, an alternating code and two short pulse schemes. The estimates of raw electron density as a function of altitude shown in Fig. 4 were obtained from one of the short pulse schemes. The spatial resolution is 3.1 km and the time resolution is 10 s. The enhancements in electron density in the EISCAT data in Fig. 4 provide clear evidence of electron precipitation. This, together with magnetic fluctuations and PI2 waves seen by the IMAGE and SAMNET chains of magnetometers, indicates that a substorm onset occurred around 20:00 UT, about 15 min before the FAST overhead pass of Tromsø. In particular, the electron density data in Fig. 4 exhibits bursts of precipitation associated with substorm onset, starting from 20:13 UT. The electron density values during these bursts are persistantly above $5 \cdot 10^{11}\,\mathrm{m}^{-3}$, with the highest electron density reaching $2 \cdot 10^{12}\,\mathrm{m}^{-3}$. Kolesnikova et al. (2002) suggested that this was important in making the artificial Alfvén wave amplitudes large enough to be detected by FAST.

Finally, analysis of the ground-based Kilpisjarvi Pulsation Magnetometer data during the period of modulated heating indicated that a strong 3 Hz wave was present in all compo-

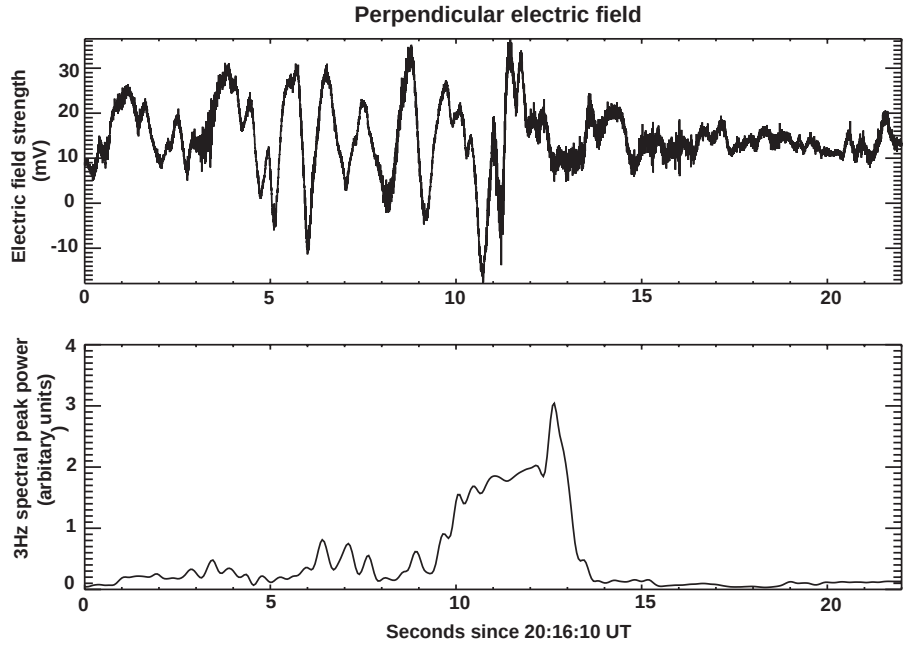

Fig. 5. Panel **(a)** shows the electric field component perpendicular to the magnetic field for a slightly wider time window to that shown in panel (a) of Fig. 3. Panel **(b)** is a sliding FFT with window width 4.0 s and slip increment 0.05 s.

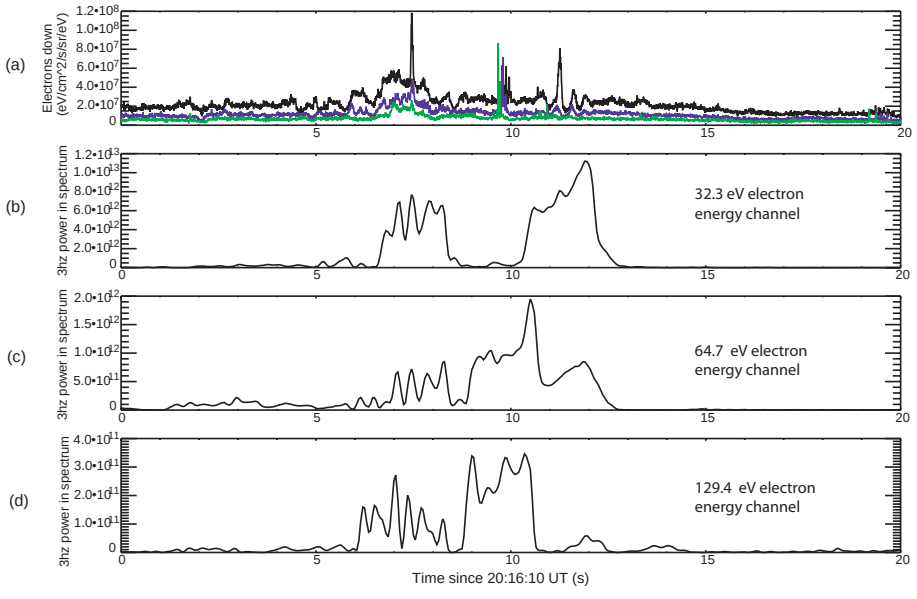

Fig. 6. SESA electron flux downward data from FAST on 8 October 1998. Panel **(a)** shows the raw flux signals (from Fig. 3 panel b), with the 32.3, 64.7 and 129.4 eV energy channels plotted in black, blue and green, respectively: 3 Hz components from the sliding FFTs for the 32.3 eV, 64.7 eV and 129.4 eV channels in panels **(b)**, **(c)** and **(d)**, respectively.

nents of the magnetic field while the heater output was modulated at 3 Hz (Wright et al., 2002). These observations are all consistent with an interpretation suggested by Robinson at al. (2000) that field-guided Alfvénic ULF waves were launched by the modulated currents in the E-region heated layer.

3 Time series analysis of the FAST data

Although a 3 Hz signature has been referred to by Robinson et al. (2000) and also in the previous section, no attempt has yet been made to establish the precise spectral content of the data in Fig. 3. In order to achieve this, a Fast Fourier Transform (FFT) was applied to a sliding window for each of the time series. This produced an estimate of the time dependence of the amplitude of the 3 Hz signals. The results for electric field, where a 4.0 s window was utilised, are displayed in Fig. 5 and those for the downward differential electron energy flux, where a 2.0 s window was used, are displayed in Fig. 6. A standard Hanning window (Lynn, 1984) was used to minimize the number of terms in the frequency response of the window. This is effectively a raised cosine bell function applied to 10% of the data points at each edge of the window. The window was moved along the time series by 0.05 s increments. In Fig. 5, the data time series

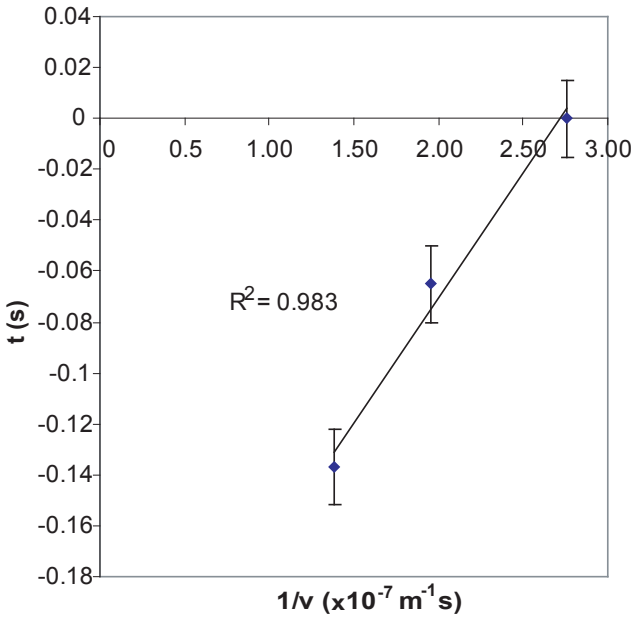

Fig. 7. Reciprocal velocity corresponding to each electron channel against lag time for interval 2 shown in pink on Fig. 3.

for the electric field is plotted in the upper panel, and in the lower panel the power (in arbitrary units) at the point in the frequency spectrum corresponding to the 3 Hz peak (binned with bandwidth of 0.5 Hz) is plotted against the time of the associated sliding window midpoint. Time is measured in seconds after 20:16:10 UT in each case. A similar procedure is carried out for the electron flux data in Fig. 6, except that the 3 Hz power is plotted in separate panels for each energy channel.

The results in Fig. 5 (lower panel) indicate that the amplitude of the 3 Hz component in the electric field spectrum was only enhanced during the 4 s interval already identified above. Of course, due to the usual compromise between spectral and temporal resolution inherent in Fourier methods, the time resolution of this data is limited by the 4-s time window used. This was chosen, somewhat arbitrarily, to provide a frequency resolution of slightly better than 10% of the centre frequency, giving (3.0 ± 0.25) Hz. However, the method does provide convincing evidence for the onset of the stimulated 3 Hz signal in the electric field, which constitutes the local detection of the upward propagating 3 Hz Alfvén wave by the FAST satellite. Similar evidence for 3 Hz signals in the 3 energy channels of the upward electron fluxes is also exhibited in the lower 3 panels of Fig. 6. However, the situation is far more complicated, because the data is more "burst-like" than the electric field data and will inevitably be broader band. Consequently, any strong short duration feature will contribute to the 3 Hz spectral component. The clearest evidence for the 3 Hz artificial oscillations is seen in the 32.3 eV channel. The 3 Hz amplitude is high in interval 2 of the artificial event. There is also a strong 3 Hz component in the natural event prior to interval 1, as expected. The other

Table 1. Time lags from FAST data (top row) calculated from the electron flux downward energy channels centred at 32.3 eV, 64.7 eV and 129.4 eV for interval 2, 20:16:20–20:16:22 on 8 October 1998

Energy channels (eV)	32.3 & 64.7	64.7 & 129.4	32.3 & 129.4
Time lags from data (sec)	0.065	0.075	0.137

two energy channels exhibit a clear diminution in 3 Hz power with increasing energy in interval 2, as might be expected from inspection of the time series data. However, there is also evidence of an increase in 3 Hz power with increasing energy for the artificial burst in interval 1. The origin of this relationship for interval 1 is not yet clear.

The broadband (or otherwise) nature of the frequency spectra for the above events was also investigated. This was done by examining more bins in the frequency spectrum. As a result, it was found that the signals associated with the electric field oscillations throughout intervals 1 and 2 (see Fig. 3), together with the downward fluxes during interval 2, were all essentially narrow band with a peak at 3 Hz. On the other hand, the downward flux burst seen in interval 1 was broader band, as might be expected from its shorter duration. The natural wave signals detected by FAST prior to the intervals 1 and 2 (for example, the burst of up-going and down-going electrons at 20:16:17 UT, which shows no velocity dispersion) tended to be broader band than artificial heating events.

Finally, the time lags between the oscillations in the different energy channels have been estimated. This was done by taking the cross-correlations of sections of the filtered time series. These are shown in Table 1. The lags obtained are similar to those found by Kolesnikova et al. (2002), who reported the lags between different channels to each be $\sim$0.05 s, by taking single peaks in the signal. A simple idealised way of interpreting this dispersion is to assume that the acceleration region is localised at a single point at a fixed distance above the spacecraft. A plot of the time lags as a function of the reciprocal of the particle velocities for the energy channels involved should then give a straight line, whose slope yields the distance from the acceleration. Figure 7 illustrates such a plot and indeed it provides a good straight-line fit. However, as is clear, the straight-line fit is not perfect, and a range of distances lie within the error bars of the data. The results are consistent with an acceleration region location and spread of (3400 ± 150) km altitude.

4 Interpretation of the downward electron flux data

According to ideal MHD theory, Alfvénic ULF waves propagate along the field lines with negligible lateral dispersion; hence, the perpendicular electric field oscillations seen by FAST may be interpreted as the direct detection of the 3 Hz shear Alfvén wave. However, the signatures in the down-

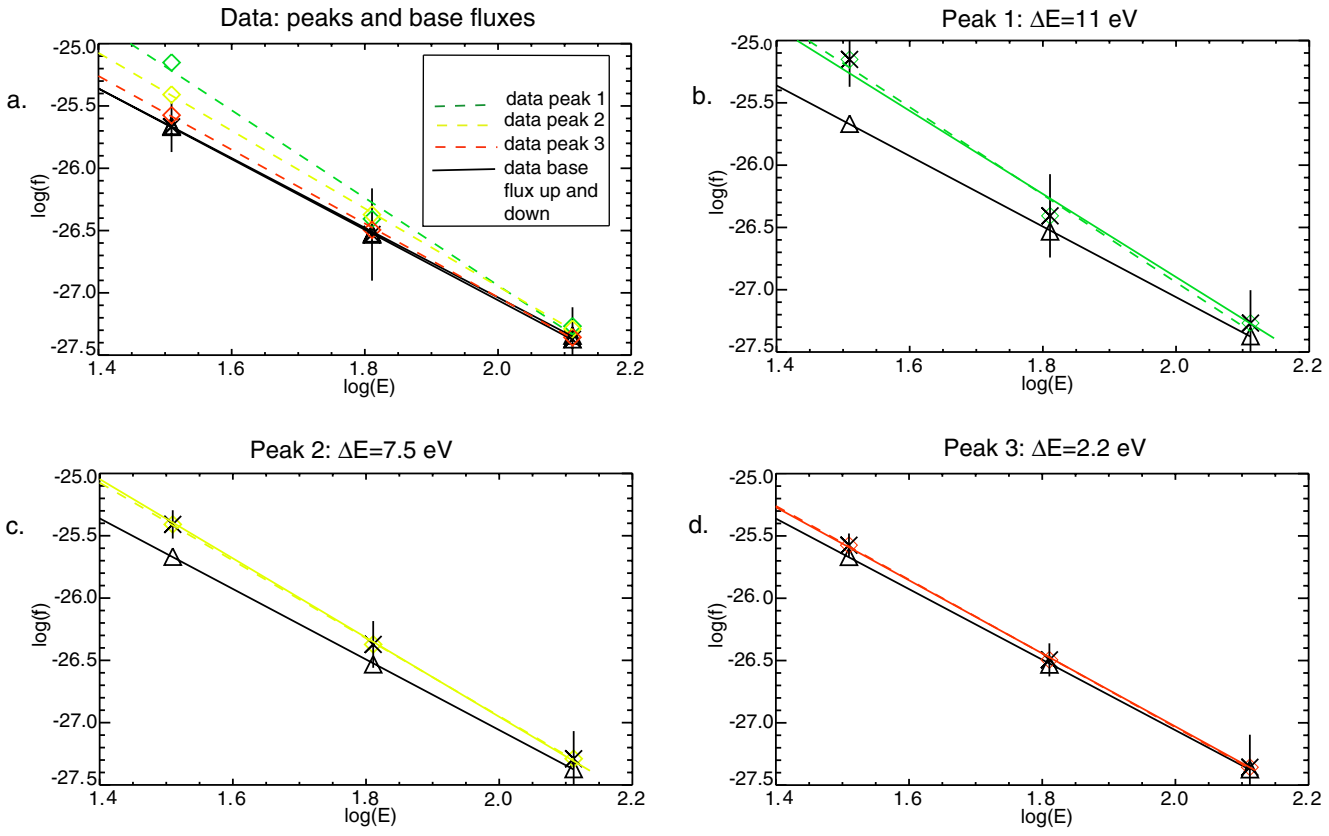

Fig. 8. Peaks in the downward differential electron energy flux data from the FAST satellite (dashed least-squares regression lines) compare well to the theoretical energy shift ΔE that electrons would have after travelling through a region of localised parallel electric field (solid colour lines) for a power law energy distribution. Panel **(a)** shows data points for each peak in the signal, with the log of the phase space density plotted against the log of the electron energy, with the associated least-squares regression line (dashed lines). Uncertainty in the base flux data points (black triangles), due to the signal noise amplitude, are shown as error bars on panel (a). Panels **(b)–(d)** show the phase space density expected by shifting the power law particle distribution from the base level (black solid line) by the ΔE displayed above each panel (solid coloured lines). Uncertainty in the peak phase space density data points (coloured diamonds), are shown on panels (b), (c), and (d) for peaks 1, 2 and 3, respectively.

ward electron flux energy channels require careful modelling, since their velocity dispersion suggests that the electrons were not energised near the satellite but from a region hundreds of km above it. A magnetic field-aligned electric field that causes an increase in velocity for downward precipitating electrons can be obtained when electron inertia effects are included in the ideal MHD theory for Alfvén waves (Robinson, 2000). It is this parallel electric field that oscillates with the passing of the ULF wave, which can accelerate the electrons from low energies to higher energy and less populated positions in the particle distribution. This is seen in the FAST electron flux data as amplitude increases and decreases at a frequency of 3 Hz as the Alfvén wave cycle progresses. This process is illustrated schematically in Fig. 1. However, the nature of the parallel electric field and the resulting potential drop along the field line need to be considered. Kolesnikova et al. (2002) assumed an idealized exponentially increasing field-aligned electric potential with altitude, obtained by solving the differential equation for an Alfvén wave propagating in an inhomogeneous plasma. The electric potential φ is assumed to vary with altitude z above altitude z_1 (altitude of FAST at 2550 km), and time t, according to the expression

$$\varphi(z,\ t) = \varphi(z_1) \exp\left(\frac{z - z_1}{H}\right) \cos\ \omega t, \qquad (1)$$

where H is the characteristic scale height of the plasma density inhomogeneity (520 km), and ω is the angular frequency of the 3 Hz Alfvén wave. $\varphi(z_1)$, the potential amplitude at altitude z_1, varies across the flux tube as the satellite passes though the (approximately Gaussian-shaped) cross field distributions in the upper IAR. This produces the different energy changes, as a function of time or horizontal position, observed in the FAST electron flux data. The exponential growth holds up to an altitude of about 4000 km when the hot plasma population starts to dominate the density variation with height. This forms the upper boundary of the IAR. This picture is consistent with our result, as mentioned previously in Sect. 3, that the region where the majority of the acceleration effect occurs is effectively localised within a nar-

row height range, with a width along the field line of about 300 km. This is comparable to the scale length of the plasma density inhomogeneity in the exponential model. Thus, significant acceleration only occurs as electrons pass through a region whose width is 300–500 km at the upper boundary of the IAR. Since the particles observed by the FAST instruments have energies of 32 eV and above, the time taken to pass through this narrow region is much shorter than the wave period. This allows for a further simplification in that the explicit time dependence in φ can be ignored for the short transit period of the main acceleration region.

The interpretation of the differential electron energy flux oscillations observed in the FAST data, in terms of this localized upward parallel electric field, will now be considered. The basic idea is as follows. When downward moving electrons pass through a quasi-static potential drop, the particle energy distribution is shifted according to

$$f(E) \rightarrow f(E + \Delta E), \tag{2}$$

where $f(E)$ is the phase space density and ΔE is the energy gained in crossing the potential drop across the acceleration region. $f(E)$ was obtained by dividing the DEF amplitude by the square of the channel central energy.

Kolesnikova et al. (2002) estimated the effect of the modulated parallel electric fields on the electron fluxes for the above events by assuming the electron distribution at the acceleration height to be a drifting Maxwellian. These authors fitted the background flux levels for the lowest 2 energy channels in the upward and downward electron fluxes to an isotropic Maxwellian with density $1.6 \cdot 10^6\,\mathrm{m}^{-3}$ and temperature 18.5 eV. However, the Maxwellian distribution that Kolesnikova et al. (2002) obtained using just 4 points from the background flux levels does not yield consistent results for the peaks in the flux data for all of the peaks in all of the electron energy channels. In particular, it is found that the amplitude of the flux oscillations in the lowest energy channel are significantly higher than would be consistent with the Maxwellian distribution. In the present study, the electron energy distribution was investigated by considering the base fluxes for all 6 upward and downward electron energy channels available from FAST (12 data points used at multiple points in the time series). This showed that a power law provides a significantly better fit to the data. Furthermore, the energy shift associated with the potential drops have a much greater effect on the fluxes in the lowest energy channels than Maxwellians do, and it was found that the flux variations across all of the energy channels were well predicted by the power law distribution. Details of the power law fits are given below.

If the particle distribution follows a power law as

$$\frac{f(E)}{f(E_0)} = \left(\frac{E}{E_0}\right)^n, \tag{3}$$

where E_0 is a constant, then the observed fluxes can be obtained by shifting the power law particle distribution by ΔE given in Eq. (2). Figure 8 illustrates how the power law particle distribution can be used to obtain a consistent fit to all of the peaks in all of the electron energy channels. The peaks are denoted by numbers 1 to 3, going left to right in Fig. 3; the times for peaks 1, 2 and 3 are approximately 20:16:21:20, 20:16:21:60 and 20:16:21:90, respectively. Panel (a) of Fig. 8 is a log-log plot of the least-squares regression lines through the energy distribution functions of the base and peak fluxes (peaks 1, 2 and 3 coloured green, yellow and red, respectively) as a function of electron channel energy observed in the lowest 3 electron energy channels. The base flux is the mean flux level in each channel at the time of the 3Hz oscillation. The value of n for the base flux regression line gradient is –2.8. The y-error bars in each panel arise from estimates of the noise amplitude in the flux signals. Panel (b) shows the data points (triangles) for the base flux downward, and the least-squares regression line (coloured black). The data points for peak 1 are shown in green diamonds, with a green dashed least-squares regression line. The base flux energies were then increased by increments in ΔE until the constructed particle distribution (solid green line) most closely matched the data regression line (dotted green line) for peak 1. The same method was used to obtain ΔE for peaks 2 and 3 shown in panels (c) and (d), respectively. The ΔE values (see Eq. 2) obtained were 11, 7.5 and 2.2 eV for peaks 1, 2 and 3, respectively, shown in Fig. 8. The ΔE values vary across the flux tube traversed by FAST in a manner which is consistent with a Gaussian function of width $\sim$10 km, with r-squared value of 0.989. This is particularly encouraging because this validates the theory outlined in Robinson et al. (2000) that the parallel electric field distribution across the outgoing edge of the heated flux tube is Gaussian-like. These potential drops across the 300 km acceleration region indicate that the parallel electric field strengths were of the order of 10^{-2} mVm^{-1}.

5 Conclusion

In this paper the electric field and electron flux data from instruments on board the FAST satellite that captured an artificial ULF wave injection event have been analysed. Spectral analysis has shown that a coherent 3 Hz signature was detected in the above data time series, within a flux tube that mapped back to the artificial ionospheric source produced by the Tromsø heater. The energy dispersed downward flux data was also analysed in detail and was found to be consistent with the existence of a localised region of oscillating parallel electric fields associated with the up-going artificial ULF wave. The acceleration region was located at around 850 km above the spacecraft (at around 3400 km) and extended approximately 300 km along the field line. This had the effect of periodically accelerating the suprathermal electrons towards the ionosphere. It was also found that the energy distribution function that best fit the mean flux data and the oscillating component was, in contrast to a previously assumed Maxwellian, a power law. The electric field amplitudes found from fitting this simple model to the measured flux

oscillation amplitudes were of the order of $10^{-2}\,\mathrm{mVm}^{-1}$, which is consistent with the model values of Kolesnikova et al. (2002).

Acknowledgements. Topical Editor G. Chanteur thanks P. Stubbe and K. Lynch for their help in evaluating this paper.

Topical Editor G. Chanteur thanks P. Stubbe and K. Lynch for their help in evalutating this paper.

References

Borisov, N. and Stubbe, P.: Excitation of longitudinal (field-aligned) currents by modulated HF heating of the ionosphere, J. Atmos. Terr. Phys., 59, 1973–1989, 1997.

Carlson, C. W., Pfaff, R. F., and Watzin, J. G.: The Fast Auroral SnapshoT (FAST) mission, Geophys. Res. Lett., 25, 2013–2016, 1998.

Chaston, C. C., Carlson, R. E., Ergun, R. E., and McFadden, J. P.: Field-aligned electron acceleration by Alfvén waves in the aurora: observations and modelling, Eos Trans., AGU, 9 May 2000 Supplement, 81, 379, 2000.

Chaston, C. C., Carlson, C. W., Peria, W. J., Ergun, R. E., and McFadden, J. P.: FAST observation of inertial Alfvén waves in the dayside aurora, Geophys. Res. Lett., 26, 647–650, 1999.

Ivchenko, N., Marklund, G., Lynch, K., Pietrowski, D., Torbert, R., Primdahl, F., and Ranta, A.: Quasiperiodic oscillations observed at the edge of an auroral arc by Auroral Turbulence 2, Geophys. Res. Lett., 26, 3365–3368, 1999.

James, H. G., Inan, U. S., and Rietveld, M. T.: Observations on the DE 1 spacecraft of ELF/VLF waves generated by an ionospheric heater, J. Geophys. Res., 95, A8, 12 187–12 195, 1990.

Kimura, I., Stubbe, P., Rietveld, M. T., Barr, R., Ishida, K., Kasahara, Y., Yagitani, S., and Nagano, I.: Collaborative experiments by Akebono satellite, Tromsø ionospheric heater, and European incoherent scatter radar, Radio Sci., 29, 23–37, 1994.

Kolesnikova, E., Robinson, T. R., Davies, J. A., Wright, D. M., and Lester, M.: Excitation of Alfvén waves by modulated HF heating of the ionosphere, with application to FAST observations, Ann. Geophysicae, 20, 57–67, 2002.

Lynn, P. A.: An Introduction to the Analysis and Processing of Signals, Macmillan, 1984.

Lysak, R. L.: Generalised model of the ionospheric Alfvén resonator, Auroral Plasma Dynamics, (Ed) Lysak, AGU, Washington, D. C., Geophys. Monogr. Ser., 80, 121–128, 1993.

Rishbeth, H. and Williams, P. J. S.: The EISCAT ionospheric radar: the system and its early results, Q. J. R. Astr. Soc., 26, 478–512, 1985.

Robinson, T. R., Strangeway, R. J., Wright, D. M., Davies, J. A., Horne, R. B., Yeoman, T. K., Stocker, A. J., Lester, M., Rietveld, M. T., Mann, I. R., Carlson, C. W., and McFadden, J. P.: FAST observations of ULF waves injected into the magnetosphere by means of modulated RF heating of the auroral electrojet, Geophys. Res. Lett., 27, 3165–3168, 2000.

Stubbe, P. and Kopka, H.: Modulated heating of the polar electrojet by powerful HF waves, J. Geophys. Res., 82, 2319–2325, 1977.

Stubbe, P., Kopka, H., Lauche, H., Reitveld, M. T., Brekke, A., Holt, O., Jones, T. B., Robinson, T. R., Hedberg, A., Thide, B., Crochet, M., and Lotz, H. J.: Ionospheric modification experiments in northern Scandinavia, J. Atmos. Terr. Phys., 44, 1025–1041, 1982.

Wright, D. M., Davies, J. A., Robinson, T. R., Yeoman, T. K., Lester, M., Cash, S. R., Kolesnikova, E., Strangeway, R., Horne, R. B., Rietveld, M. T., and Carlson, C. W.: The tagging of a narrow flux tube using artificial ULF waves generated by modulated high power radio waves, J. Geophys. Res., submitted, 2002.